Int. J. Heat Mass Transfer. Vol. 25, No. 11, pp. 1755–1766, 1982
Printed in Great Britain

0017–9310/82/111755–12 $03.00/0

CONVECTIVE HEAT TRANSFER IN VERTICAL CYLINDRICAL ANNULI FILLED WITH A POROUS MEDIUM

M. A. HAVSTAD and P. J. BURNS
Department of Mechanical Engineering, Colorado State University, Fort Collins, CO 80523, U.S.A.

(*Received* 23 *November* 1981 *and in final form* 19 *April* 1982)

Abstract—Convective heat transfer in the concentric vertical annulus filled with a porous medium has been investigated. Numerical results for the heat transfer are presented for moderate cylinder spacings and for high temperature differences. Perturbation results for the field variables are supplied which are valid for all cylinder spacings at low temperature differences. An asymptotic solution is given which is valid for very tall cylinders and all temperature differences. Finally, this multiplicity of solutions is consociated with a curve fit. The results are found to be in fair agreement where there is overlap in their independent variables. Furthermore, there is qualitative agreement with results for the horizontal concentric cylinders and spheres filled with a porous medium, although the dependence on the aspect ratio leads to some interesting phenomena.

NOMENCLATURE

A, aspect ratio of annulus, H/r_o;
Bi, Biot number, hr_o/k;
Da, Darcy number, K/r_o^2;
Gr, Grashof number, $g\beta\Delta T\, r_o^3/\nu^2$;
g, gravitational constant [m s^{-2}];
H, height of annulus [m];
h, convective heat transfer coefficient [W m^{-2} K^{-1}];
j, iteration counter;
K, permeability of porous media [m^2];
k, thermal conductivity [W m^{-1} K^{-1}];
Pr, Prandtl number, ν/α;
p, pressure [N m^{-2}];
Q, heat flow [W];
q, heat flux [W m^{-2}];
Ra^*, modified Rayleigh number, $g\beta\Delta TKr_o/(\nu\alpha)$;
Ra, Rayleigh number, $g\beta\Delta Tr_o^3/(\nu\alpha)$;
r, radial spatial coordinate [m];
T, dimensional temperature [K];
u, velocity component in radial direction [m s^{-1}];
w, velocity component in vertical direction [m s^{-1}];
Y, any field variable, either ψ or θ;
z, vertical spatial coordinate [m].

Greek symbols

α, thermal diffusivity [m^2 s^{-1}];
β, coefficient of cubical expansion [K^{-1}];
γ, constant of proportionality;
η, radius ratio, r_i/r_o;
θ, dimensionless temperature, $(T - T_o)/(T_i - T_o)$;
μ, absolute viscosity [N s m^{-2}];
ρ, density [kg m^{-3}];
ψ, dimensionless stream function defined in equation (9).

Subscripts

cn, convective and nondimensional;
cond, conduction alone;
i, inside;
j, iteration counter;
o, outside or "infinity";
total, conduction and convection.

Superscripts

', nondimensional quantity;
*, modified.

1. INTRODUCTION

THE INCREASING relative cost of energy has led engineers to more closely examine measures which may decrease energy use. Thermal insulation will continue to find increased use as engineers seek to reduce costs. This work investigates heat transfer in porous thermal insulation applied within vertical cylindrical annuli in order to provide insight into the mechanisms of this form of energy transport and to enable engineers to use insulation more efficiently. In particular, design engineers require relationships between heat transfer, geometry and boundary conditions which can be utilized in cost–benefit analyses to determine the amount of insulation that will yield the maximum return on investment.

Since so very little literature exists dealing with free convective flow in a porous media between concentric cylinders, free convective flow in enclosures containing only a simple fluid will first be discussed. The subject of free convection in enclosures completely filled with a porous medium will then build upon this base with a discussion focusing first on the rectangular geometry and then on annuli.

The subject of free convection in enclosures containing only simple fluids was reviewed by Ostrach [1].

Ostrach emphasized the differences between internal and external free convective flows and gave considerable attention to the simplifying assumption often considered in the literature that, for the internal flow region, a central isothermal core exists and this region is enclosed by a boundary-layer type flow. Of all the free convection enclosure problems, horizontal cylindrical geometries are probably the most studied. Powe, Carley and Bishop [2] reviewed all experimental work for free convection in horizontal isothermal concentric cylinders. They summarized the data and its discrepancies, and then reduced the flow in the annuli to four basic regimes and thereby generated a starting point for theoretical work.

Powe, Carley and Carruth [3] reported the results of a finite difference solution for free convection in horizontal cylindrical annuli. Their work was able to predict the transition from steady to unsteady flow and their results showed excellent qualitative agreement overall. This work has been recently extended by other authors [4].

Natural convection in enclosed vertical annuli filled with "simple" fluids has been treated, though not nearly as thoroughly as horizontal annuli. Gershunig [5] attempted an analytical treatment. He solved the governing equations by decoupling momentum and energy by assuming that velocity terms do not interact with the energy equation. This approach was unsatisfactory. Later, Beckmann [6] suggested that vertical annuli could be correlated to vertical plates with limited success. Then Nagendra *et al.* [7] utilized a double boundary layer model proposed by Emery and Chu to obtain acceptable agreement between theory and experiment. Three different correlations for different categories of annuli were presented and agreement with available experimental data was within 6%.

In summary, natural convection in horizontal annuli filled with a simple fluid is well understood. The works of Powe *et al.* [2, 3] give a firm base to the fundamental aspects and subsequent works treat only very specialized extensions. In contrast, vertical annuli deserve further treatment and have not been examined in the complete way [2, 3] as have horizontal annuli.

The investigation of heat transfer in enclosures containing porous media began with the experimental work of Verschoor and Greebler [8]. These researchers used an evacuable guarded hot plate apparatus to determine the relative importance of radiation, conduction and convection in enclosures filled with air and thermal insulation. Verschoor and Greebler demonstrated that gas conduction is the primary transport mechanism at low Rayleigh numbers and that radiation contributes little to the overall heat transfer in practical building applications (as predicted by their analytic work). Verschoor and Greebler were followed by several other investigators interested in porous media heat transfer in rectangular enclosures [9–12]. In particular, Bankvall [13–15] has published a great deal of practical work concerning heat transfer by natural convection in rectangular enclosures completely filled with porous media.

Results published by Burns, Chow and Tien [16] describe a porous media heat transfer flow with a rectangular geometry which is less idealized than the preceding works. Additionally, infiltration is allowed. They present results of Nusselt number as a function of several parameters and find that for high infiltration rates the dominant heat transfer mechanism is due to the enthalpy change of the fluid blown through the enclosure.

Natural convection in porous media with cylindrical geometries is not nearly as well studied as the rectangular counterpart. The governing equations and flow field are significantly more complex in cylindrical coordinates. Caltagirone [17] and Brailovskaya *et al.* [18] have published results for horizontal geometries, but little in these works concerns heat transfer in practical flow regimes for thermal insulation. Tien and Bejan [19] published results for heat transfer between concentric horizontal cylinders with different end temperatures. They found the heat transfer to depend on the Rayleigh number, the geometry, and the conduction properties of the wall. Burns and Tien [20] also published theoretical work concerning heat transfer in horizontal concentric cylinders and spheres.

In summary, heat transfer in porous media has received considerable attention recently, and the specific topic of transport in thermal insulation has been approached for several fundamental geometries, though usually with idealized boundary conditions. There is a dearth of work, however, in the instance of vertical cylindrical annuli.

2. THE GOVERNING EQUATIONS

2.1. *Basic equations and geometry*

The governing equations expressing conservation of mass, momentum and energy for the problem at hand are

$$\nabla \cdot \mathbf{u} = 0, \tag{1}$$

$$\mathbf{u} = \frac{-K}{\mu}(\nabla p + \rho \mathbf{g}), \tag{2}$$

$$\mathbf{u} \cdot \nabla T = \alpha \nabla^2 T. \tag{3}$$

Equation (1) is the incompressible form of the continuity equation and equation (2) is Darcy's law for steady fluid flow in a porous medium. Darcy's law applies for Reynolds numbers (based on pore diameter) less than one. Equation (3) is a steady state formulation of the principle of conservation of energy with the thermal conductivity assumed to be constant. Viscous dissipation is negligible while radiation is approximately accounted for by selecting an appropriate value of the experimentally determined thermal conductivity (which includes radiation).

The geometry under consideration is shown in Fig. 1. In dimensional form, the important geometrical parameters of the problem are the inner and outer

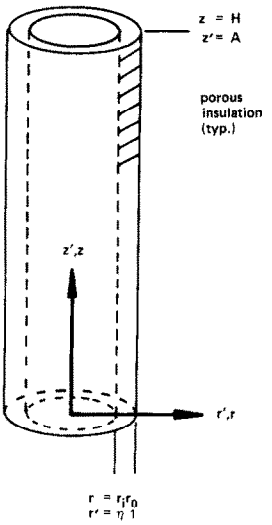

FIG. 1. The physical system.

cylinder radii, r_i and r_o, respectively, and the cylinder height, H. In nondimensional form, the radius ratio, $\eta = r_i/r_o$, and the aspect ratio, $A = H/r_o$, are the important geometrical parameters. The nondimensional radial variable, r', varies from η to 1, and the vertical variable, z', varies from zero to A. The two nondimensional geometrical parameters, the boundary conditions, and the modified Rayleigh number will determine the heat transfer and the flow field.

Equations (1)–(3) can be written in cylindrical coordinates to take advantage of the angular symmetry of the problem. The following equations are then obtained:

$$\frac{\partial}{\partial r}(ru) + r\frac{\partial}{\partial z}(w) = 0, \tag{4}$$

$$u = -\frac{K}{\mu}\frac{\partial p}{\partial r}, \tag{5}$$

$$w = -\frac{K}{\mu}\left(\frac{\partial p}{\partial z} + \rho g\right), \tag{6}$$

$$u\frac{\partial T}{\partial r} + w\frac{\partial T}{\partial z} = \alpha\left[\frac{1}{r}\frac{\partial}{\partial r}\left(r\frac{\partial T}{\partial r}\right) + \frac{\partial^2 T}{\partial z^2}\right]. \tag{7}$$

The variables in the above four equations are nondimensionalized as follows:

$$u' = \frac{u}{\alpha/r_o},\ w' = \frac{w}{\alpha/r_o},\ r' = r/r_o,\ z' = z/r_o,$$
$$\theta = \frac{T - T_o}{T_i - T_o},\ p' = \frac{p}{\alpha\mu/K} + \frac{\rho_o g z}{\alpha\mu/K}. \tag{8}$$

Pressure is eliminated by taking the partial derivative of equation (5) with respect to z and the partial derivative of equation (6) with respect to r. By introducing a nondimensional stream function defined as

$$\frac{-1}{r'}\frac{\partial\psi}{\partial r'} = w'\frac{\partial\psi}{\partial z'} = r'u' \tag{9}$$

the continuity equation is automatically satisfied and the variables u' and w' are replaced by the single variable ψ. Finally, using the Boussinesq approximation and dropping the primes, the following coupled pair of equations are obtained:

$$r\frac{\partial}{\partial r}\left(\frac{1}{r}\frac{\partial\psi}{\partial r}\right) + \frac{\partial^2\psi}{\partial z^2} = -Ra^* r\frac{\partial\theta}{\partial r}, \tag{10}$$

$$\frac{1}{r}\frac{\partial}{\partial r}\left(r\frac{\partial\theta}{\partial r}\right) + \frac{\partial^2\theta}{\partial z^2} = \frac{1}{r}\frac{\partial\psi}{\partial z}\frac{\partial\theta}{\partial r} - \frac{1}{r}\frac{\partial\psi}{\partial r}\frac{\partial\theta}{\partial z} \tag{11}$$

where Ra^* is the modified Rayleigh number defined by

$$Ra^* = g\beta\Delta T r_o K/(\alpha\nu). \tag{12}$$

The modified Rayleigh number expresses how vigorously the flow is thermally driven compared to how firmly motion is resisted and can be given as a product of three nondimensional parameters as follows:

$$Ra^* = Gr\,Pr\,Da, \tag{13}$$

Ra^* being used for brevity and simplicity.

The horizontal boundaries are nonconducting and the inner vertical boundary is held at a constant elevated temperature, T_i. In the perturbation solution, the outer boundary is held at a constant lower temperature, T_o. In the numerical and asymptotic solutions, the outer vertical boundary is allowed to convect to the ambient at T_o by virtue of a constant heat transfer coefficient, h. As the vertical annulus is defined to be an enclosure, or sealed, the edges of the enclosure must constitute a streamline. Hence, the boundary conditions may be stated mathematically as

$$\begin{aligned} &\psi\,(\text{boundaries}) = 0,\\ &\frac{\partial\theta}{\partial z} = 0 \text{ at } (z = 0 \text{ and } A, \text{ all } r),\\ &\theta(\eta, z) = 1,\\ &\theta(1, z) = 0 \text{ (perturbation solution)},\\ &\frac{\partial\theta}{\partial r} = -Bi\,\theta \text{ (asymptotic and numerical solutions)}, \end{aligned} \tag{14}$$

where

$$Bi = hr_o/k \tag{15}$$

and h is a heat transfer coefficient for convection outside the cylinder and k is the stagnant thermal conductivity of the porous medium.

Solutions to the governing equations are desired over the full range of practical values of the parameters of the problem. Hence the radius ratio varies from 0.1 to 0.9 and the aspect ratio varies from 0.5 to 20. The range of the modified Rayleigh number is determined using experimental data previously collected. Fournier and Klarsfeld [21] report that the permeability of fibrous insulation varies from 2×10^{-10} to $200 \times 10^{-10}\,m^2$. They also report that an effective thermal conductivity, which includes the effects of gas conduction, solid conduction and radiation varies from 3.2×10^{-2} to $5.0 \times 10^{-2}\,W^{-1}\,m^{-1}\,K^{-1}$. Using these values for the permeability and thermal conductivity, the well known properties for air, insulation thicknesses up to 1/3 m, and temperature differences up to 70 K, the modified Rayleigh number may vary as follows in practical insulation applications:

$$0 < Ra^* < 150. \tag{16}$$

Equations (10) and (11) are nonlinear, coupled partial differential equations. After failing to obtain an exact analytical solution, approximate analytical and numerical results were sought. Perturbation techniques valid for low Rayleigh numbers were attempted to garner information when the geometry approaches limiting values and numerical difficulty is encountered. An asymptotic solution was obtained that is valid when the enclosure is tall and narrow for very high Rayleigh numbers where, again, numerical difficulty is encountered. Finally, the gaps were bridged with numerical results. These solutions will be described in the ensuing sections.

3. PERTURBATION SOLUTION

In the problem at hand, a parameter perturbation [22] is performed in which the modified Rayleigh number is perturbed from zero, a value for which the full problem solution (the log law conduction profile) is known. To do this, θ and ψ are assumed to be of the form

$$\theta = \theta_0 + Ra^*\theta_1 + Ra^{*2}\theta_2 + \ldots, \tag{17}$$

$$\psi = \psi_0 + Ra^*\psi_1 + Ra^{*2}\psi_2 + \ldots. \tag{18}$$

These series are substituted into the governing equations (10) and (11) and the boundary conditions, equations (14). As the modified Rayleigh number tends to zero all terms not containing θ_0 and ψ_0 drop out. The following pair remains:

$$r\frac{\partial}{\partial r}\left(\frac{1}{r}\frac{\partial\psi_0}{\partial r}\right) + \frac{\partial^2\psi_0}{\partial z^2} = 0, \tag{19}$$

$$\frac{1}{r}\frac{\partial}{\partial r}\left(r\frac{\partial\theta_0}{\partial r}\right) + \frac{\partial^2\theta_0}{\partial z^2} = 0. \tag{20}$$

The solutions to the above pair are

$$\psi_0 = 0, \tag{21}$$

$$\theta_0 = \ln r/\ln \eta. \tag{22}$$

Higher order terms are generated similarly. ψ_1 was obtained by standard separation of variables techniques. A homogeneous solution is obtained and the inhomogeneous term was developed by inspection. ψ_1 is given by

$$\psi_1 = \frac{1}{2\ln\eta}[z^2 + Az] + r\sum_{n+1}^{\infty}\sin\frac{n\pi z}{A}\left[\frac{-K_1(\mu)}{I_1(\mu)}I_1(\mu r) + K_1(\mu r)\right]D'_n + \left[\frac{-K_1(\mu\eta)}{I_1(\mu\eta)}I_1(\mu r) + K_1(\mu r)\right]D_n \tag{23}$$

where

$$\mu = \mu_n = \frac{n\pi}{A}, \tag{24}$$

$$D_n = \frac{\dfrac{2}{\ln\eta}\dfrac{A^2}{n^3\pi^3}(\cos n\,\pi - 1)}{K_1(\mu) - \dfrac{K_1(\mu\eta)}{I_1(\mu\eta)}I_1(\mu)} \tag{25}$$

and

$$D'_n = \frac{\dfrac{2}{\eta\ln\eta}\dfrac{A^2}{n^3\pi^3}(\cos n\,\pi - 1)}{K_1(\mu\eta) - \dfrac{K_1(\mu)}{I_1(\mu)}I_1(\mu\eta)}. \tag{26}$$

The equation for θ_1 is

$$\frac{1}{r}\frac{\partial}{\partial r}\left(r\frac{\partial\theta_1}{\partial r}\right) + \frac{\partial^2\theta_1}{\partial z^2} = \frac{1}{r}\frac{\partial\psi_1}{\partial z}\frac{\partial\theta_0}{\partial r} \tag{27}$$

θ_1 was obtained using the same techniques used for ψ_1 and is given by

$$\theta_1 = (\ln r)^2\left(-\frac{A_1^2 z}{2} + \frac{A_1^2 A}{4}\right) + \sum_{n=1}^{\infty}\cos\frac{n\pi z}{A}[E_n\ln r\,I_0(\mu r) + B_n\ln r\,K_0(\mu r)] + \sum_{n=1}^{\infty}C_{3n}\left[Y_0(\beta_n r) - \frac{Y_0(\beta_n)}{J_0(\beta_n)}J_0(\beta_n r)\right]\cosh\beta_n z + \sum_{n=1}^{\infty}C_{4n}\left[Y_0(\beta_n r) - \frac{Y_0(\beta_n)}{J_0(\beta_n)}J_0(\beta_n r)\right] \times [-\cosh(\beta_n z) - \tanh(\beta_n A)\sinh(\beta_n z)] + \sum_{n=1}^{\infty}C_{7n}\left[K_0(\mu r) - \frac{K_0(\mu)}{I_0(\mu)}I_0(\mu r)\right]\cos\mu z. \tag{28}$$

Here the constants μ_n, β_n, E_n, B_n, A_1, C_{3n}, C_{4n} and C_{7n} are functions of η and A. Solutions for θ_2 and ψ_2 were not obtained because the solutions for θ_1 and ψ_1 are so complex that the equations for θ_2 and ψ_2 would be extremely difficult to solve. Additionally, it was found to be very expensive to obtain the eigenvalues and to sum the series in equations (23) and (28). The extrapolation to ψ_2 and θ_2 indicated that we couldn't afford to perform the computations even if we had the solutions. The velocities, u_1 and w_1, can be obtained using equation (19) and are given, together with the constants in equations (28) in ref. [24].

The Nusselt number, Nu, defined as follows:

$$Nu = \frac{\dot{Q}_{\text{total}}}{\dot{Q}_{\text{cond}}} = \ln \eta \int_0^A r \frac{\partial \theta}{\partial r} \mathrm{d}z \tag{29}$$

is one when calculated using the first two terms of equation (17). Thus, the first order contribution to the heat transfer is zero because of the vertically antisymmetric nature of θ_1. This has been observed in the past [20] with the result that at low Rayleigh numbers, the heat transfer varies at least quadratically with Rayleigh number.

The absence of Nusselt number results for the perturbation solution led to a comparison of temperature fields to assess the accuracy of the method. The numerical results were taken as ground truth. Since the cost of a complete error analysis was untenable, two cases were considered: $Ra^* = 30$ and $Ra^* = 50$ for $Bi = \infty$, $\eta = 0.5$ and $A = 5$. At $Ra^* = 35$ and $r = 0.65$ (where the errors are representative averages of the field), the error varies from 0.0005% at $z = 0.15$ to 8% at $Z = 2.5$. At $Ra^* = 50$, the error varies from 1.3% at $z = 0.15$ to 15.1% at $z = 5$. It appears, therefore, that the perturbation solution is accurate enough for engineering purposes below $Ra^* = 35$.

4. ASYMPTOTIC SOLUTION

For a vertical annulus completely filled with a porous medium the governing equations are greatly simplified as we let $A \to \infty$. Indeed, this should be a valid approximation for many practical insulation systems. Because the height of the annulus becomes infinite, there can be no change in fundamental quantities with height. All derivatives with respect to z go to zero. The governing pair, equation (10) and (11), becomes

$$\frac{1}{r}\frac{\partial^2 \psi_A}{\partial r^2} - \frac{1}{r^2}\frac{\partial \psi_A}{\partial r} = -Ra^* \frac{\partial \theta_A}{\partial r}, \tag{30}$$

$$\frac{1}{r}\frac{\partial}{\partial r}\left(\frac{r \partial \theta_A}{\partial r}\right) = 0. \tag{31}$$

The appropriate boundary conditions are:

$$\psi_A(\eta, z) = 0,$$

$$\psi_A(1, z) = 0,$$

$$\theta_A(\eta, z) = 1,$$

$$\theta_A(1, z) = \frac{-1}{Bi}\frac{\partial \theta_A}{\partial r}(1, z). \tag{32}$$

The heat flow boundary condition at $r = 1$ is more general than that posed in the perturbation problem. The boundary conditions stated in equations (32) reduce to the perturbation boundary conditions in the limit as the Biot number tends to infinity. The temperature of the outer cylinder now assumes a value greater than zero depending upon the internal flow and the Biot number. The solutions to equations (30)–(32) are as follows:

$$\psi_A = +\frac{Ra^* Bi r^2}{2(1 - Bi \ln \eta)}\left[\ln r - \frac{1}{2}\right] + C_1 \frac{r^2}{2} + D_1, \tag{33}$$

$$\theta_A = \frac{1}{1 - Bi \ln \eta}[-Bi \ln r + 1] \tag{34}$$

$$C_1 = \frac{-Ra^* Bi}{1 - Bi \ln \eta}\frac{\eta^2 \ln \eta - \frac{\eta^2}{2} + \frac{1}{2}}{\eta^2 - 1} = \frac{-Ra^* Bi}{1 - Bi \ln \eta}[C_2], \tag{35}$$

$$D_1 = \frac{Ra^* Bi}{2(1 - Bi \ln \eta)}\left[\frac{1}{2} + \frac{\eta^2 \ln \eta - \frac{\eta^2}{2} + \frac{1}{2}}{\eta^2 - 1}\right] \tag{36}$$

Using the definition of ψ, given by equation (9), w_A can be obtained. The result is

$$w_A = -\frac{Ra^* Bi \ln r}{1 - Bi \ln \eta} - C_1. \tag{37}$$

Using w_A and θ_A it is possible to estimate the convective contribution to the heat transfer in annuli with a large but not infinite aspect ratio, A. There are a number of ways in which this can be done. This work employs a method successfully introduced by Batchelor [23]. In short, the technique assumes that the nondimensional convective contribution to heat transfer in "tall" annuli is proportional to the convected energy, i.e.

$$\dot{Q}_{\text{cn}} = \gamma \int_\eta^1 w_A \theta_A \, 2\pi r \mathrm{d}r \tag{38}$$

where the constant of proportionality, γ, is to be determined by comparison to other solution techniques or experimental data. Evaluation of the integral is complicated but the result obtained, after substituting into the definition of the Nusselt number is

$$Nu_A = 1 + \frac{Ra^*\gamma}{A} \times \left[\frac{\frac{\eta^2 \ln^2 \eta}{2} + (C_2 + 1)\left[-\frac{1}{4} - \frac{\eta^2}{2}\left(\ln \eta - \frac{1}{2}\right)\right]}{\ln \eta}\right] \quad (39)$$

for $Bi = \infty$, and

$$Nu_A = 1 - \frac{\gamma Ra^*}{A} \times \left\{\left[\frac{Bi}{1 - Bi \ln \eta}\left(\frac{\eta^2 \ln^2 \eta}{2}\right) - \frac{C_2(1 - \eta^2)}{2(1 - Bi \ln \eta)}\right] + \left[\frac{Bi}{1 - Bi \ln \eta} + \frac{C_2 Bi}{1 - Bi \ln \eta} + \frac{1}{1 - Bi \ln \eta}\right]\left[-\frac{1}{4} - \frac{\eta^2}{2}\left(\ln \eta - \frac{1}{2}\right)\right]\right\} \quad (40)$$

for $Bi < \infty$.

Equation (40) readily reduces to equation (39) as the Biot number tends to ∞. The relations for Nu_A are valuable as they allow prediction of heat transfer from simple analytical expressions for large aspect ratio geometries. The shape of Nu_A is very similar to the shape of the Nu (η) plots presented in the numerical results section, indicating good qualitative agreement.

Quantitative agreement is obtained by using least squares methods in comparing Nu_A to numerical solution results. Least square methods enable a selection of a value for γ which minimizes the variation of the Nusselt number. This procedure has been applied to over 50 numerical results for Nusselt numbers of 5 and greater and γ has been determined to be 0.57.

The Nusselt number results obtained from the asymptotic and numerical schemes have been compared for all $A \geq 1$. For the asymptotic results, the maximum error is observed for the minimum values of η and the smaller values of A at all Ra^*. The results agree to better than 11% for all cases where both $\eta > 0.1$. Almost all results agree to within 5%. The variation of error is illustrated for the representative case of $Ra^* = 100$ and $A = 5$ as follows – the error varies smoothly with η from 0.5% at $\eta = 0.9$ to 5.3% at $\eta = 0.2$.

5. NUMERICAL SOLUTION

This work utilizes the two previously discussed analytic efforts as well as a finite difference scheme to obtain results for heat transfer as a function of geometry, Biot number, and modified Rayleigh number. Finite differences were employed because the boundary conditions were unambiguous and smooth and the finite difference method is known to be successful on very similar problems, specifically natural convection in enclosures and natural convection in porous media filled enclosures [20].

5.1. *The finite difference approximation scheme*

Equations (10) and (11) were formulated in central difference form. A regular grid was used. Boundary mirroring was used to satisfy the adiabatic conditions and second order one-sided differencing was used to calculate temperature gradients on the vertical boundaries. This formulation has been utilized in a successive over-relaxation scheme. In this scheme, θ and ψ are given initial approximate values and the scheme solves for θ and ψ successively until a determined residual is reached.

In the investigation described above, runs using grids as large as 50 × 50 were sometimes used, but for the bulk of the output, grids between 16 × 16 and 30 × 30 were used. Fifteen exploratory cases indicated that accuracy is determined by several factors besides grid size. The values of A, η, and Ra^* all combine in a complex manner to determine the grid size required to obtain a given accuracy. Most results at $Ra^* \leq 50$ were accurate to within about 2%; the more inaccurate runs are those where the Nusselt number peaks versus η. Results at $Ra^* = 150$ are within about 8% of the converged value, and again, only the results near the maximum Nusselt number are less accurate, though all are accurate to at least 12%. All results at $Ra^* = 100$ are accurate to within 8%. The series of runs was prohibitively expensive, and the results shown are converged to the maximum limit allowed by our budget.

The convergence properties of the successive over-relaxation scheme were investigated by fixing η, A, Ra^* and the grid size and varying the convergence parameter, *RESMAX*. *RESMAX*, the maximum normalized change in the temperature on the stream function over every grid point is given by

$$RESMAX = \left[1 - \frac{Y_j(r, z)}{Y_{j-1}(r, z)}\right]_{\max}. \quad (41)$$

When the change between the new and old values of the temperature or stream function normalized with the old value, is smaller than *RESMAX*, then the convergence criterion is satisfied. The temperature at an arbitrary grid point in the upper center of the enclosure was converged when *RESMAX* was equal to 1.0×10^{-4}. Thus in all subsequent runs *RESMAX* was set to 1.0×10^{-5} and the temperature and stream function at every grid point were forced to satisfy the convergence criterion.

Figures 2–5 display results of the numerical scheme for a Biot number of infinity. These results are tabulated in ref. [24]. The Nusselt number is presented as a function of radius ratio, η, with the aspect ratio, A, as a parameter for Rayleigh numbers of 35, 50, 100 and 150. Numerical results are shown as solid points while asymptotic results are shown as open points. Asymptotic results are shown for $A \geq 2$. The asymptotic approximation is invalid for small A. Indeed, it is surprising that the asymptotic results agree as well as they do even at $A = 2$. Due to budget limitations (the results shown herein cost several thousands of dollars) the numerical results are not as plentiful as is desirable.

This is somewhat ameliorated by the curve fit presented later.

In each graph, the Nusselt number tends to one, the pure conduction value, as η tends to 0 and 1. The former result is due to the fact that as η goes to zero, the area for heat liberation tends to zero. The latter result is due to the fact that as η goes to unity, the conductive resistance goes to zero. The heat transfer increases with modified Rayleigh number. This must occur because, as previously described, the modified Rayleigh number is the driving force for convective heat transfer. The Nusselt number dependence on aspect ratio A is presented most clearly for $Ra^* = 35$. For η's near 0 and 1 the Nu dependence on A appears as a fairly simple inverse power law dependence but for η between 0.2 and 0.6 the dependence is more complex. In this region, Nu increases and then decreases with decreasing A for a given η, so that the η for which Nu is a maximum for each A moves from about $\eta = 0.2$ for $A = 10$ to $\eta = 0.45$ for $A = 0.5$. This result may be explained by considering the flow geometry. For smaller A, the pathlines are long in the horizontal direction and short in the vertical direction, where heat transfer occurs. Long pathlines make the flow rate low and decrease the convective heat transfer. As A gets small, then, Nu goes to unity. However, as A gets large, the convective heat transfer approaches a limit because fluid rising next to the inner wall cannot get hotter than the inner wall itself. Conduction increases with increasing A so that as A gets very large Nu goes to one once again. Hence, Nu vs A must go through a maximum.

Figures 6 and 7 depict streamlines and isotherms generated by the numerical scheme for $Ra^* = 100$, $A = 2.0$ and $\eta = 0.2$. The isotherms show little resemblance to the vertical isotherms of the conduction solution or the nearly vertical result of the perturbation solution. As in the perturbation solution, the streamlines encircle a point that is shifted to the outside of the annulus. However, the streamlines are no longer symmetrical about $z = A/2$. The vortex or central flow point is shifted noticeably above $z = A/2$ and there is a decidedly higher flow rate in the upper outside corner and the lower inside corner. The symmetry of the perturbation solution forced the vortex to be centered along $z = A/2$. Additional terms in the perturbation solution, if well behaved, should move the vortex center upward and outward to its correct position. The upper inside and lower outside regions are relatively stagnant. As fluid rises along the inner vertical wall and warms, a higher pressure region develops in the upper inside corner. The flow must turn toward the outside away from the corner, leaving a large fairly stagnant region. As the flow approaches the outside wall it cools and descends abruptly. Another high pressure stagnant zone develops in the lower outside region and the flow turns toward the inside as it falls. In the lower inside region the fluid warms and abruptly begins to rise. The isotherms depicted in Fig. 8 can be explained with the aid of the flow. In the upper region the flow affects the conduction temperature the

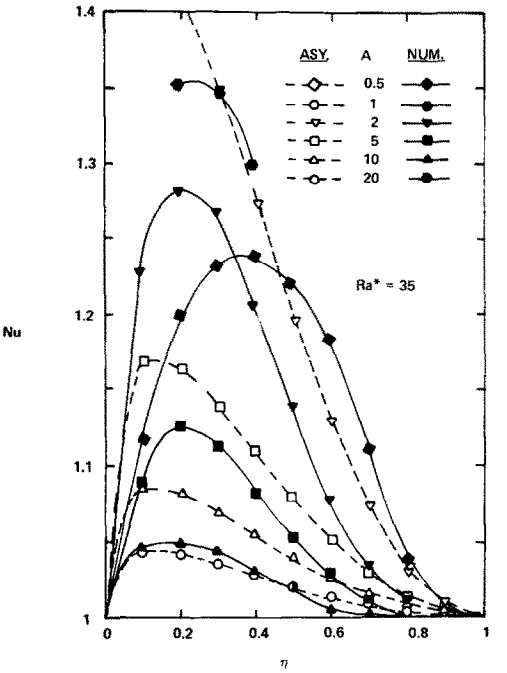

FIG. 2. The variation of Nusselt number with radius ratio for $Ra^* = 35$.

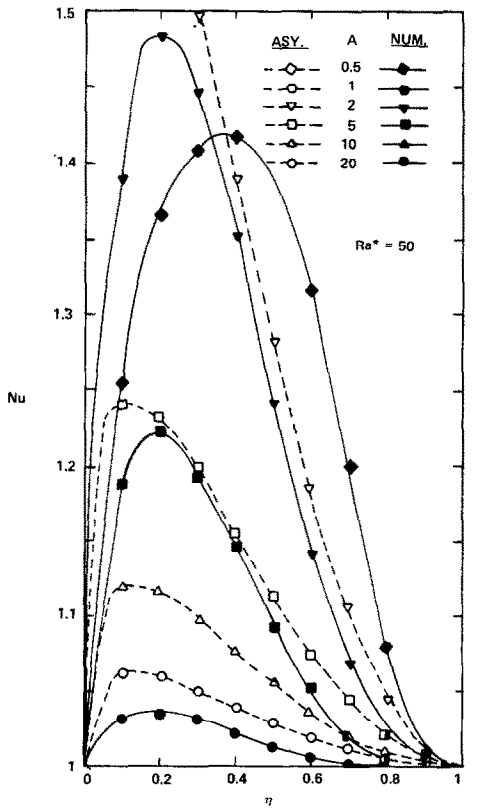

FIG. 3. The variation of Nusselt number with radius ratio for $Ra^* = 50$.

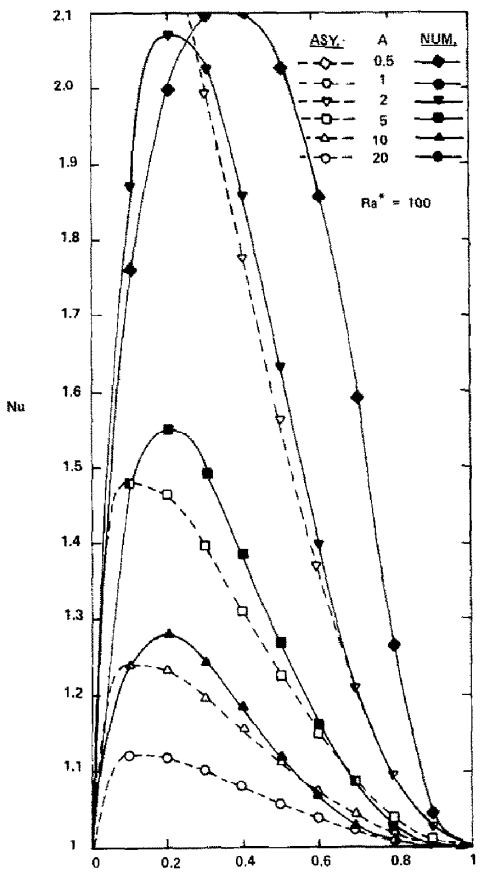

FIG. 4. The variation of Nusselt number with radius ratio for $Ra^* = 100$.

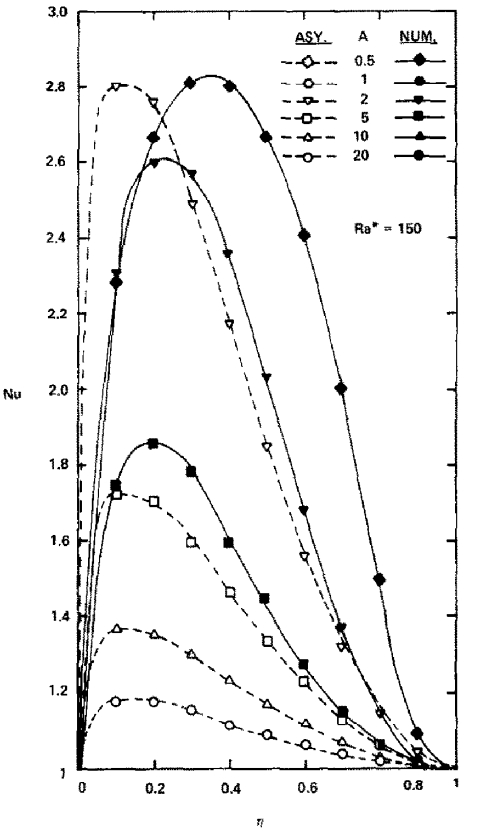

FIG. 5. The variation of Nusselt number with radius ratio for $Ra^* = 150$.

same way blowing from the inner to outer wall would. The isotherms must shift toward the outside. Where the conduction profile would have given $\theta = 0.80$, blowing gives a larger value, for example 0.85 or 0.9. The temperature field in the lower region of the enclosure resembles blowing from the outer to inner wall and the isotherms shift toward the inner wall.

The numerical scheme allows either the convective or the isothermal boundary condition to be applied at the outer vertical boundary. The results for an isothermal outer boundary have been presented. Cost considerations have limited the number of finite Biot results, but as there are more than fifty of these results, there are enough to obtain a good idea of the effects. The majority of the results are at Biot numbers of 30 or larger, where the Nusselt number is more than ninety percent of its value for $Bi = \infty$. Lower Biot number results were extremely expensive, partly because the algorithm's first guess was poor in this region and partly because the algorithm's convergence properties were weaker with the finite Biot number boundary condition. The results indicate that decreasing the Biot number decreases the Nusselt number. An infinite Biot number, or an isothermal outer wall, implies an infinite heat transfer coefficient on the outer vertical wall. An infinite h is required to keep the entire wall at the

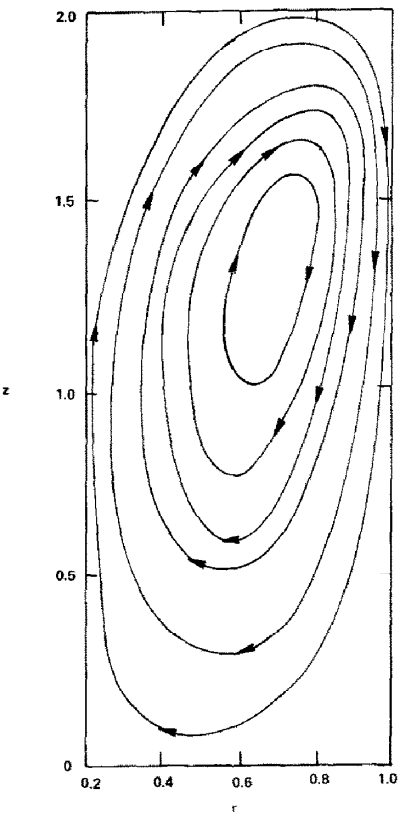

FIG. 6. Streamlines for $\eta = 0.2$, $A = 2$, and $Ra^* = 100$.

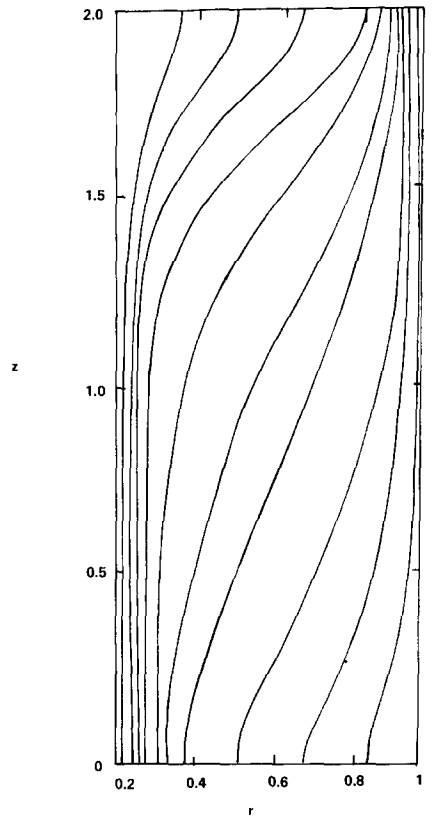

FIG. 7. Isotherms for $\eta = 0.2$, $A = 2$, and $Ra^* = 100$.

temperature of the surrounding fluid, the fluid outside of the vertical annulus. As h decreases from infinity, the outer wall grows warmer because it does not transfer heat to the surrounding fluid as well. An increase in the outer wall temperature reduces the effective modified Rayleigh number in the enclosure and therefore must decerease the heat transfer because the Rayleigh number is the parameter which drives the convective heat tranfer in the enclosure. As the outer wall warms up when the Biot number decreases from infinity, it does not remain isothermal. The outer wall warms more near the top of the annulus because the fluid in the upper region inside the annulus is warmer and transfers heat to the outer wall more strongly as it vigorously impinges on the surface. This result causes the outer boundary as well as the fluid in the annulus to be thermally stratified. Thermal stratification opposes the fluid motion in the enclosure.

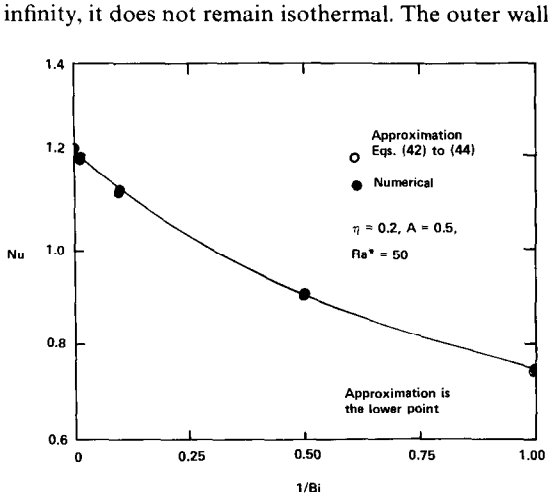

FIG. 8. The variation of the Nusselt number with the inverse of the Biot number.

The dependence of the Nusselt number on the Biot number is illustrated in Fig. 8. The independent variable is $1/Bi$. The decrease in Nusselt with Biot number is not appreciable until the Biot number is less than 50. Thus, for Biot numbers of 50 to ∞, the heat transfer is very near the isothermal outer wall heat transfer. For Biot numbers less than about 4, Nu is less than 1 because it is still normalized with the isothermal outer wall conduction solution. As the Biot number gets very small, it decreases the heat transfer less and less because the temperature difference across the enclosure is reduced resulting in a decrease in the flow. Thus, the internal heat transfer tends to the pure conduction solution as the Biot number is decreased. Additionally, stratification becomes more pronounced which further inhibits flow.

A method has been developed which uses the $Bi = \infty$ numerical results to predict the $Bi < \infty$ numerical results to within about 2%. The heat transfer in the annulus can be expressed in nondimensional form as

$$\frac{(1 - \theta_0)Nu_\infty}{\ln \eta} = -Bi\,\theta_0 \tag{42}$$

where Nu_∞ is the Nusselt number for an infinite Biot number evaluated at a modified Rayleigh number reduced to account for the increased outer wall temperature, θ_0. Finite Biot number results can be approximated to within 2% using this relation by following the procedure outlined below.

Choose η, A, Ra^* and Bi. After guessing θ_0, reduce the modified Rayleigh number to account for the increased outer wall temperature with the following relation:

$$Ra^*_{red} = Ra^*\,(1 - \theta_0). \tag{43}$$

Using Ra^*_{red}, interpolate in the infinite Biot results for a Nusselt number prediction. Use this Nu_∞ value to derive a new θ_0 from equation (42). With the new θ_0, a new reduced modified Rayleigh number can be obtained and the process can be iterated until θ_0, Ra^*_{red} and Nu_∞ converge. Nu_{Bi} is then calculated using

$$Nu_{Bi} = Nu_\infty\,(1 - \theta_0). \tag{44}$$

This has been done and is shown as the open points on Fig. 8. The results converged after only 3 iterations to values within 2% of the numerical results. In fact there is so much overlap that the open points (lower) can barely be discerned from the solid points.

Least squares methods have been used to approximate the Nusselt number's dependence on η, A and Ra^* with simple functions for design purposes. Both the A and Ra^* dependence were fit well to simple

power law functions. The η dependence was fitted to

$$a_1[\eta(1-\eta)]^{a_2}e^{a_3\eta}. \quad (45)$$

The specific function is given in its entirety in the Conclusions section. Results for these correlations have been compared to the numerical results. The agreement is always within 5%.

Some results from the asymptotic solution (open points) are compared to numerical solution results in Figs. 2–5. The asymptotic solution is accurate to 6% for all η greater than 0.3 and $A > 2$. The asymptotic solution is poor at smaller η, though it tends to the appropriate limit as $\eta \to 0$ but allows reasonable results for $\eta \geq 0.3$. For $A < 2$, the asymptotic solution diverges from the numerical results. This is to be expected because $A < 2$ violates the basic assumptions in the approximation.

6. CONCLUSIONS

The governing equations for free convection in vertical cylindrical annuli were formulated in differential form as the first step towards obtaining useful information regarding heat transfer in thermal insulations. The governing equations were then reduced to a coupled pair of nonlinear equations involving a single parameter, the modified Rayleigh number. The application of the boundary conditions introduced the radius ratio, the aspect ratio and the Biot number and the problem was then one involving five parameters. Because the critical modified Rayleigh number is zero, and solutions were sought for modified Rayleigh numbers between 0 and 150.

Perturbation methods were applied and yielded first term corrections for the stream function and temperature to the pure conduction case. Unfortunately, higher order terms were too difficult to obtain and the first term corrections could not give results for Nusselt number due to antisymmetry about $z = A/2$. However, useful results for the flow field were obtained.

Asymptotic methods yielded useful results for $A \geq 5$ and $\eta > 0.2$. Qualitative agreement was not obtained for $\eta < 0.2$ because of the assumptions required for the asymptotic technique. However, as many practical problems involve an $A \geq 5$, the method's results are quite useful.

Numerical methods generated results for a wide range of η, A and Ra^*. Some results for Biot numbers between 1 and 500 were also obtained. Simple correlation equations were developed to relate the Nusselt number to η, A and Ra^*. A simple iterative technique for obtaining results at finite Biot numbers from results for $Bi = \infty$ was presented.

Several results of the present work display some provocative similarities to two important preceding works. The Nusselt number results of Burns and Tien [20] for concentric horizontal annuli show a very similar radius ratio dependence. The curve fit for the numerical results has a nearly identical form despite a great difference in flow field between the two problems. However, many of the constants are very different. The Nusselt number's dependence on Ra^*, though, is an exception. In both problems, the Nusselt number seems to go as Ra^{*2} at the lower Rayleigh numbers but as low as $Ra^{*1.1}$ at the higher Rayleigh numbers.

The results of Batchelor [23] for free convection of a simple fluid between vertical plates are similar to those of the present problem in several respects. In both works, the first term of the perturbation solution did not contribute to heat transfer, and in both problems, the Rayleigh or modified Rayleigh number dependence goes as the second power for the small (less than 50) Rayleigh numbers.

The preceding work leads to the following conclusions:

(1) The Nusselt number, and therefore the heat transfer, in vertical concentric cylindrical annuli containing porous insulation depends on radius ratio, aspect ratio, modified Rayleigh number and Biot number, all nonlinearly.

(2) The dependence of the Nusselt number on the modified Rayleigh number is nearly quadratic for $Ra^* \leq 50$, as was expected when the terms in Ra^* in the perturbation solution did not contribute to heat transfer by virtue of their antisymmetry about $z = A/2$.

(3) For a given Rayleigh number, a critical height occurs at which the Nusselt number is a maximum. This occurs because the Nusselt number is normalized with conduction, $A/\ln \eta$. Conduction increases linearly with A, while convection approaches a limiting value and therefore increases much more slowly for larger A's.

(4) A relation of the following form fits the $Bi = \infty$ results well:

$$Nu = 1 + a_1[\eta(1-\eta)]^{a_2}e^{-a_3\eta}\frac{Ra^*}{A^{a_5}}$$

$$\text{for } A \geq 1,\ 0 < Ra^* < 150 \text{ and all } \eta \quad (46)$$

$$a_1 = 0.2196,$$

$$a_2 = 1.3337,$$

$$a_3 = 3.7020,$$

$$a_4 = 0.92958,$$

$$a_5 = 1.1682.$$

The correlation for the Nusselt number can be extended to the use where $Bi < \infty$ by using the procedure outlined in equations (42)–(44). Results were shown to be accurate to about 2%.

(5) For Biot numbers of 50 or larger, the heat transfer is within 5% of the $Bi = \infty$ value. However, Biot numbers as low as 0.05 are required to simulate natural convection on the outer vertical wall for all practical applications.

(6) The Nusselt number is a maximum for a given A and Ra^* at a particular η. This result is due to the fact that Nu must go to unity both as η goes to zero, because the area for heat liberation tends to zero, and as η goes to one, because the conductive resistance tends to zero. A maximum must therefore occur at an

intermediate value of η. The value of η at the maximum Nusselt number is observed to be $(\eta)_{max} = 0.25$ for $A > 1$ while $(\eta)_{max}$ increases continuously with decreasing A for $A < 1$.

(7) For $Bi = \infty$, no critical insulation thickness exists at which heat transfer is a maximum or minimum. Despite the existence of maximum Nusselt numbers, heat transfer does not peak because of the variation of the conduction solution with η. For Biot numbers less than infinity, a maximum is expected to exist as occurs in the well known problem with closed cell or solid insulation.

Further studies should utilize a more sophisticated algorithm to enable investigation of problems with more realistic boundary conditions i.e. lower Biot numbers. The temperature dependence of the properties should also be taken into direct consideration.

Acknowledgements—The authors wish to express their gratitude to Drs Fred Smith, Robert Haberstroch and Richard Loehrke for their support and aid with the analysis.

REFERENCES

1. S. Ostrach, Natural convection in enclosures, in *Advances in Heat Transfer*, Vol. 8, pp. 161–227. Academic Press, New York (1972).
2. R. E. Powe, C. T. Carley and E. H. Bishop, Free convective flow patterns in cylindrical annuli, *Trans. Am. Soc. Mech. Engrs*, Series C, *J. Heat Transfer* **91,** 310–314 (1969).
3. R. E. Powe, C. T. Carley and S. L. Carruth, A numerical solution for natural convection in cylindrical annuli, *Trans. Am. Soc. Mech. Engrs*, Series C, *J. Heat Transfer* **93,** 210–220 (1971).
4. S. N. Singh and J. M. Eliot, Free convection between horizontal concentric cylinders in a slightly thermally stratified fluid, *Int. J. Heat Mass Transfer* **22,** 639–645 (1979).
5. Z. Gershunig, *Dokl. Akad. Nauk SSSR*, No. 4, **86,** 687–694 (1952).
6. M. Jakob, *Heat Transfer*, Vol. 1. J. Wiley, New York (1952).
7. H. R. Nagendra, M. A. Tirunarayanan and A. Ramachandran, Free convection heat transfer in vertical annuli, *Chem. Engng Sci.* **25,** 605–610 (1970).
8. J. D. Verschoor and P. Greebler, Heat transfer by gas conduction and radiation in fibrous insulation, *Trans. Am. Soc. Mech. Engrs* 961–968 (1952).
9. A. Rubin and S. Schweitzer, Heat transfer in porous media with phase change, *Int. J. Heat Mass Transfer* **15,** 43–59 (1972).
10. P. H. Holst and K. Aziz, Transient three dimensional natural convection in confined porous media, *Int. J. Heat Mass Transfer* **15,** 72–89 (1972).
11. F. A. Morrison, Transient multiphase multicomponent flow in porous media, *Int. J. Heat Mass. Transfer* **16,** 2331–2341 (1973).
12. R. J. Ribando and K. E. Torrance, Natural convection in a porous medium: effects of confinement, variable permeability and thermal boundary conditions, *Trans. Am. Soc. Mech. Engrs*, Series C, *J. Heat Transfer* **98,** 42–48 (1976).
13. C. G. Bankvall, Natural convective heat transfer in insulated structures, Lund Inst. of Tech. Report 38 pp. 1–149 (1972).
14. C. G. Bankvall, Heat transfer in fibrous materials, *J. Test. Eval.* **3,** 235–243 (1973).
15. C. G. Bankvall, Guarded hot plate apparatus for the investigation of thermal insulations. Document D5, National Swedish Building Research (1972a).
16. P. J. Burns, L. C. Chow and C. L. Tien, Convection in a vertical slot filled with porous insulation, *Int. J. Heat Mass Transfer* **20,** 919–926 (1977).
17. J. P. Caltagirone and A. Majtabi, Convection between two coaxial cylinders in a laminar permanent regime, *Int. J. Heat Mass Transfer* **21,** 261–268 (1978).
18. V. A. Brailovskaya, G. B. Pbtrazhitsky and V. I. Polezhaer, On the effect of convective heat exchange on thermal-insulation properties of permeable porous interlayers, in *Heat Transfer in Buildings*. Hemisphere, New York (1982).
19. A. Bejan and C. L. Tien, Natural convection in horizontal space bounded by two concentric cylinders with different end temperatures, *Int. J. Heat Mass Transfer* **22,** 919–927 (1979).
20. P. J. Burns and C. L. Tien, Natural convection in porous media bounded by concentric spheres and horizontal cylinders *Int. J. Heat Mass Transfer* **22,** 929–938 (1979).
21. D. Fournier and S. Klarsfeld, Some recent experimental data on glass fiber insulating materials and their use for a reliable design of insulations at low temperatures, *ASTM STP 544*, p. 223–242 (1974).
22. M. Van Dyke, *Perturbation Methods in Fluid Mechanics*. The Parabolic Press, Stanford (1975).
23. G. K. Batchelor, Heat transfer by free convection across a closed cavity between vertical boundaries at different temperatures, *Q. Appl. Math.* **12,** 209–233 (1954).
24. M. A. Havstad, Free convective heat transfer between vertical concentric cylinders containing porous insulation, MS thesis, Colorado State University (1980).

CONVECTION THERMIQUE DANS UN ESPACE ANNULAIRE VERTICAL EMPLI D'UN MILIEU POREUX

Résumé—On étudie la convection thermique dans un espace annulaire vertical et concentrique, empli d'un milieu poreux. Des résultats numériques sont présentés pour des espaces modérés et pour des différences de température élevées. Des résultats de perturbation pour les variables de champ sont fournis pour tous les espaces de cylindre et pour des faibles différences de température. Une solution asymptotique est donnée qui est valable pour des grands cylindres et n'importe quelle différence de température. Les résultats sont en bon accord là ou il y a recouvrement des variables indépendantes. De plus il y a un accord quantitatif avec les résultats connus pour les cylindres concentriques horizontaux et les sphères remplis avec un milieu poreux, et la dépendance au rapport de forme conduit à des phénomènes intéressants.

KONVEKTIVER WÄRMETRANSPORT IN EINEM MIT PORÖSEM MATERIAL GEFÜLLTEN SENKRECHTEN ZYLINDRISCHEN RINGSPALT

Zusammenfassung—Es wurde der konvektive Wärmetransport in einem mit porösen Material gefüllten vertikalen Ringspalt untersucht. Numerische Ergebnisse für den Wärmetransport in zylindrischen Räumen mit mäßigem Wandabstand und hohen Temperaturunterschiedenwerden angegeben. Störungslösungen für die Feldgrößen werden ermittelt, die für alle Wandabstände bei kleinen Temperaturunterschieden gültig sind. Eine asymptotische Lösung wird angegeben, die für sehr große Zylinder und alle Temperaturdifferenzen gültig ist. Schließlich wird diese Vielzahl von Lösungen durch eine Ausgleichskurve zusammengefaßt. Es wurde gefunden, daß die Ergebnisse in guter Übereinstimmung sind, wo sich ihre unabhängigen Variablen überlappen. Außerdem besteht qualitative Übereinstimmung mit veröffentlichten Ergebnissen für ebene konzentrische Zylinder und mit porösem Material gefülte Kugeln, obwohl die Abhängigkeit vom Längen/Durchmesser-Verhältnis zu einigen interessanten Phänomenen führt.

КОНВЕКТИВНЫЙ ТЕПЛОПЕРЕНОС В ВЕРТИКАЛЬНЫХ ЦИЛИНДРИЧЕСКИХ КОЛЬЦЕВЫХ КАНАЛАХ, ЗАПОЛНЕННЫХ ПОРИСТОЙ СРЕДОЙ

Аннотация—Проведено исследование конвективного теплопереноса в концентрическом вертикальном кольцевом канале, заполненном пористым веществом. Численные результаты по теплопереносу приведены для случаев небольших зазоров между цилиндрами и больших разностей температур. Представлены рассчитанные по теории возмущений поля основных переменных, которые применимы для любых зазоров между цилиндрами и небольших разностей температур. Дано также асимптотическое решение, справедливое для цилиндров большой высоты при любых разностях температур. Кроме того, вся совокупность решений подтверждается совпадением с экспериментальной кривой. Показано, что результаты хорошо согласуются в том случае, когда имеет место наложение независимых переменных. Кроме того, получено качественное согласие с известными результатами для горизонтальных концентрических цилиндров и сфер, заполненных пористой средой, причем зависимость процесса от отношения радиуса к высоте цилиндра приводит к некоторым интересным явлениям.